

# A self-consistent approach to the Wigner-Seitz treatment of soliton matter

Urban Weber\* and Judith A. McGovern†

*Theoretical Physics Group, Department of Physics and Astronomy  
University of Manchester, Manchester, M13 9PL, U.K.*

## Abstract

We propose a self-consistent approach to the treatment of nuclear matter as a crystal of solitons in the Wigner-Seitz approximation. Specifically, we use a Bloch-like boundary condition on the quarks at the edge of a spherical cell which allows the dispersion relation for a given radius to be calculated self-consistently along with the meson fields; in previous work some ansatz for the dispersion relation has always been an input. Results in all models are very sensitive to the form of the dispersion relation, so our approach represents a significant advance.

We apply the method to both the Friedberg Lee model and the chiral quark-meson model of Birse and Banerjee. Only the latter shows short range repulsion; in the former the transition to a quark plasma occurs at unrealistically low densities.

24.85.+p, 12.39.Ki, 21.65.+f

Typeset using REVTeX

---

\*Current address: Institute of Experimental Physics, FR 10.2 Experimental Physics, Universität des Saarlandes, D66041 Saarbrücken

†Electronic address: j.mcgovern@man.ac.uk

## I. INTRODUCTION

It is universally accepted that nucleons are composite objects made out of quarks, and that it will eventually be necessary to include this substructure in order to successfully model all properties of nuclei and nuclear matter. For many years now there has been a program of modelling the nucleon as being primarily composed of three light relativistic quarks bound together in a localised spherical region by a mean field generated by their mutual interaction. Such soliton models have the advantage over their precursor, the MIT bag, that the structure is fully dynamical, and so its response to external probes can be calculated consistently.

Apart from the calculation of the properties of static, isolated nucleons, one of the earliest applications of soliton models was to nuclear matter. There are two main ways in which this has been done. One, which was started later but has been taken further, involves modelling the effect of the presence of other nucleons on a test nucleon by constant background fields, typically the  $\sigma$  and  $\omega$  mesons which play such an important role in quantum hadrodynamics [1]. Since these background fields will modify the soliton structure, which in turn will change the meson-nucleon coupling constants, the value of the fields for a given density can be calculated self-consistently. Such calculations may well capture the essential physics at low densities. At nuclear matter densities, however, the inter-nucleon separation is very comparable to the nucleon radius. If soliton models, in which the quark profiles fall to zero smoothly as a function of distance from the centre, are to be taken seriously, then the quark wavefunctions of different nucleons must overlap significantly. The other approach to soliton matter treats this as the dominant effect [2–7].

If nuclear matter were crystalline, we would know how to tackle the problem. Single quark energy levels would be replaced by Bloch wavefunctions, satisfying  $\psi(\mathbf{r} + \mathbf{R}) = e^{i\mathbf{k}\cdot\mathbf{R}}\psi(\mathbf{r})$  for lattice vectors  $\mathbf{R}$ . By concentrating on a single cell the Bloch condition gives boundary conditions on the wavefunction within that cell for all values of the crystal momentum  $\mathbf{k}$  within the first Brillouin zone, with the lowest energy state corresponding to  $\mathbf{k} = 0$  and an energy gap above the highest energy state. It is therefore possible to start with an approximate form of the potential, find a sufficient set of states to enable the quark density to be integrated over the band, solve for the potential generated by these quarks and then iterate until convergence is reached. While simple in principle, this would be a formidable task in practice, since the potential and wavefunctions will contain all spherical harmonics and the integration in  $\mathbf{k}$ -space is three-dimensional. The closest to realising this program which has been achieved so far was also the earliest such study. Achtzehnter *et al* [2] used the Friedberg-Lee model on a face-centred cubic lattice. However they calculated states and energies for only one direction in  $\mathbf{k}$ -space, and assumed that the dispersion relation was the same in all directions, thereby simplifying the calculation of the quark density.

However nuclear matter has no long-range crystalline order. This fact, coupled with a desire for a less cumbersome calculational method, inspired the approach that has been taken ever since, namely the use of the Wigner-Seitz approximation [8]. In their first paper Wigner and Seitz were concerned with the energy of the bottom of the band in sodium. They made the assumption that within the cell the potential is spherically symmetric, and also that the polyhedral cell boundary is well approximated by a sphere. The Schrödinger wavefunction for the state at the bottom of the band will therefore be spherically symmetric

and be flat on the boundary. (For Dirac wavefunctions, those become the conditions on the upper component.) These assumptions seem particularly suitable for soliton matter, which is not crystalline, since they do not depend on any particular lattice, but instead reflect the average isotropy of a liquid. For a full calculation, however, it is not enough to have the bottom of the band; the wavefunctions of all states in the band are required.

Most authors in the field of soliton matter have assumed that all the states in the band are also  $s$ -wave states (surprisingly, since the Bloch condition is strongly anisotropic for non-zero  $\mathbf{k}$ ) so that the dispersion relation is independent of direction. They then made a variety of assumptions about the form of the dispersion relation and the position of the top of the band. Birse *et al* [3] for instance took the top to be the state for which the upper component of the Dirac wavefunction vanishes at the cell boundary. Between these two states the dispersion relation was assumed to be a sinusoid, with  $d\epsilon/dk = 0$  at the bottom and top of the band. The quark density was built up by sampling the full band. Another assumption used has been that the width of the band is twice the difference between the energy of the isolated soliton and the energy of the bottom of the band defined as above [4]. A third is to assume that the dispersion relation is given by  $\epsilon = \sqrt{\epsilon_b^2 + k^2}$ , with the top of the band given by  $k_t = \pi/2R$  [5]. The last assumption is also used in ref. [7], where, following Wigner and Seitz's second paper, they write  $\psi_{\mathbf{k}}(\mathbf{r}) = e^{i\mathbf{k}\cdot\mathbf{r}}u_{\mathbf{k}}(\mathbf{r})$ , and then assume that  $u_{\mathbf{k}}(\mathbf{r}) = \psi_0(\mathbf{r})$ . Wigner and Seitz carefully checked this assumption—which is clearly not exact since the equation for  $u_{\mathbf{k}}(\mathbf{r})$  depends on  $\mathbf{k}$ —and found that for sodium, where the quadratic dispersion relation reflects the fact that the electrons are nearly free, the approximation was a good one. For well-separated solitons, in which the quarks remain clearly localised and the dispersion relation is likely to show pronounced flattening at the top of the band, it is unlikely to hold. Some authors have simplified still further by allowing only the states at the top or bottom of the band to be occupied. The problem with all these approaches is that the algorithm for finding the top of the band is completely ad-hoc. Furthermore the contribution of the quarks to the energy of the cell, proportional to  $\int_0^{k_t} \epsilon(k) k^2 dk$ , is dominated by the higher states, and so the results for the dependence of the energy on density are extremely sensitive to the assumptions used. None of the studies performed so far can thus be regarded as reliable guides to physics.

The current work was motivated by the desire to retain the strengths of the Wigner-Seitz approach, namely the lack of dependence on a particular lattice structure and the recognition of the approximately spherically-symmetric environment of the nucleon, but in a fashion that allows the band structure to be calculated self-consistently. We therefore propose to retain a Bloch-like boundary condition to relate the values of the wavefunction at any pair of antipodal points for points on the boundary  $\mathcal{S}$ ,

$$\psi(\mathbf{r}) = e^{2i\mathbf{k}\cdot\mathbf{r}}\psi(-\mathbf{r}), \quad \forall \mathbf{r} \in \mathcal{S}. \quad (1)$$

The closer to spherical the Brillouin zone for a particular lattice is, the closer this is to the normal Bloch condition. Essentially this is the logical continuation of the Wigner-Seitz method. Furthermore this boundary condition is also satisfied by a plane wave of momentum  $\mathbf{k}$ , and so it also holds for the quark plasma state which will be the lowest energy state at high densities. For a band based on an  $s$ -wave state, this gives the same condition for the bottom of the band,  $k = 0$ , as was used previously, namely the vanishing of the lower component

at the cell boundary (being a  $p$ -wave, the lower component is odd under  $\mathbf{r} \rightarrow -\mathbf{r}$ ). However for a given spherical potential this condition can be solved for any  $\mathbf{k}$ . If the potential is sufficiently deep, this gives a dispersion relation  $\epsilon(k)$  which turns over at a certain value of  $k$ ; this point, at which  $d\epsilon/dk = 0$ , is naturally taken as the top of the band. (The dispersion relation is of course isotropic.) The band based on the next state (with a radial node in the isolated wavefunction) will not overlap with the lowest band, and so there is a band gap. The wavefunctions will not of course be spherically symmetric, except at the bottom of the band, and so are taken as sums over partial waves. However the quark density, integrated over the direction as well as the magnitude of  $\mathbf{k}$ , *is* spherically symmetric, and so can be used to generate a new spherically symmetric potential; the process is repeated until convergence is reached. This is the first fully self-consistent calculation of soliton matter to be reported.

There are physical effects which have not been taken into account in this calculation; spurious centre of mass energy has not been subtracted nor energy due to fermi motion of the nucleons added, and the effects of one-gluon exchange or meson clouds apart from those which form the soliton have not been included—the effects which split the nucleon from the delta are absent. This is not yet a realistic model of nuclear matter, but it is a better starting point than any proposed so far.

## II. THE MODELS

Two models have been used in the current work: the Friedberg-Lee model and the chiral quark-meson model, which we will introduce briefly in turn.

The Friedberg-Lee model [9] is the prototypical soliton model, consisting only of quarks and a single scalar field,  $\sigma$ , which couples linearly to the quarks. The potential for the  $\sigma$  has an absolute minimum at a non-zero value of  $\sigma$ ,  $\sigma_v$ , which is the value the field takes in the vacuum, but in the presence of a scalar quark density the minimum of the effective potential is pushed closer to zero. While quarks can exist as free particles, with a mass  $g\sigma_v$ , it will be energetically favourable for three quarks to be localised in space in a “bag” of lower  $\sigma$ ; this is a soliton. The Lagrangian is as follows:

$$\mathcal{L} = \bar{\psi}(i\gamma^\mu\partial_\mu - g\sigma)\psi + \frac{1}{2}\partial_\mu\sigma\partial^\mu\sigma - U(\sigma), \quad (2)$$

where  $U(\sigma) = a\sigma^2/2 + b\sigma^3/3! + c\sigma^4/4! - B_{vac}$ , and results will be presented for the case  $a = 0$ ,  $b = -700.43 \text{ fm}^{-1}$ ,  $c = 10^4$  and  $g = 10.98$ , giving  $B_{vac} = 0.27 \text{ fm}^{-4}$  and  $\sigma_v = 0.21 \text{ fm}^{-1}$ . For these parameters the isolated soliton has an isoscalar r.m.s. radius of 0.83 fm, and energy of 1265 MeV.

The Friedberg-Lee model lacks chiral symmetry. This can be restored by making the  $\sigma$  field the chiral partner of the pion potential. This chiral quark-meson model was introduced by Birse and Banerjee [10] and by Kahana *et al* [11]. The Lagrangian is

$$\mathcal{L} = \bar{\psi}(i\gamma^\mu\partial_\mu + g(\sigma + i\gamma_5\boldsymbol{\tau} \cdot \boldsymbol{\phi}))\psi + \frac{1}{2}\partial_\mu\sigma\partial^\mu\sigma + \frac{1}{2}\partial_\mu\boldsymbol{\phi}\partial^\mu\boldsymbol{\phi} - U(\sigma, \boldsymbol{\phi}), \quad (3)$$

where  $U(\sigma, \boldsymbol{\phi})$  is the Mexican hat (wine-bottle) potential, quadratic in  $\sigma^2 + |\boldsymbol{\phi}|^2$ , plus a small symmetry breaking term linear in  $\sigma$  which gives explicit chiral symmetry breaking and a non-zero pion mass. Unlike the F-L model, for which soliton formation is independent of the

spin-isospin structure of the quarks, which may therefore be taken to be in the appropriate SU(6) wavefunction, spherical solutions in the chiral model require all three quarks to be in a “hedgehog” configuration,  $\chi_h = (u \downarrow -d \uparrow)/\sqrt{2}$ . The  $\sigma$  field is radially symmetric, and the pion fields have their isospin vector pointing radially outwards,  $\phi_i(\mathbf{r}) = \hat{r}_i h(r)$ . The resulting soliton is a superposition of all states with equal spin and isospin, namely the nucleon, delta and higher resonances. States of good spin and isospin must be projected out, by cranking or other methods. It is far from clear how to do this for a soliton in matter, and we here deal only with hedgehog matter in this model. We use parameters in the potential which give  $\sigma_v = f_\pi = 93$  MeV,  $m_\pi = 139$  MeV and  $m_\sigma = 1200$  MeV, and take  $g = 5.38$ , which gives a soliton energy of 1116 MeV.

### III. SOLITON MATTER: THE METHOD

For each cell radius,  $R$ , a self-consistent solution was obtained, consisting of a spherically symmetric  $\sigma$  field subject to the boundary condition  $\sigma'(R) = 0$  and quarks in states characterised by the crystal momentum  $\mathbf{k}$ , satisfying the boundary condition (1), with states evenly distributed throughout a sphere in  $\mathbf{k}$ -space of radius  $k_t$ ,  $k_t$  being the top of the band. As stressed in the introduction, the dispersion relation  $\epsilon(k)$  and  $k_t$  are themselves calculated self-consistently. If the pion field is present, its odd parity leads to the boundary condition  $h(R) = 0$ .

Details of the calculation are as follows. We start with an isolated soliton, in order to have a good approximation to the potential at large radii, and after a converged solution is found for each radius its potential is used as the initial guess for a smaller radius; thus we work inwards until the solution is finally lost.

The quark scalar density is found as follows for the F-L model. The hedgehog ansatz introduces some complications which are covered in the appendix. For a given potential, the bottom of the band is easily found by solving the Dirac equation for the  $s$ -wave state subject to the condition that the lower component vanishes at  $r = R$ . In order to have what turns out from experience to be an upper limit on the energy of the top of the band, it is useful also to find the energy of the state for which the upper component vanishes at  $R$ . The true top is typically about half way between the bottom and this upper limit. The wavefunction for non-zero  $\mathbf{k}$  will not be spherically symmetric, but a superposition of states of all angular momenta; it proves sufficient in practice to include the first 14 states. Since the boundary condition is independent of spin and axially symmetric, states with spin projection parallel and antiparallel to  $\mathbf{k}$  have the same energy; we need only consider one of them and allow for spin and isospin degeneracy separately. Thus, taking  $\mathbf{k} = k\hat{\mathbf{z}}$ , we use for our trial state

$$\psi_{\mathbf{k}}(\mathbf{r}) = \sum_{\kappa} i^{l_{\kappa}} D_{\kappa} \begin{pmatrix} u_{\kappa,\epsilon}(r) \\ i\boldsymbol{\sigma} \cdot \hat{\mathbf{r}} v_{\kappa,\epsilon}(r) \end{pmatrix} \Phi_{\kappa}^{\frac{1}{2}}(\theta, \phi). \quad (4)$$

The quantum number  $\kappa$  ( $\kappa = \pm 1, \pm 2, \dots$ ) gives the total angular momentum,  $j_{\kappa} = |\kappa| - \frac{1}{2}$  and the orbital angular momentum of the upper component,  $l_{\kappa} = \kappa$  for  $\kappa > 0$  and  $l_{\kappa} = |\kappa| - 1$  for  $\kappa < 0$ ;  $\kappa = -1$  corresponds to the  $s$ -wave state. The  $\Phi_{\kappa}^m(\theta, \phi)$  are spin-orbit functions of spin- $\frac{1}{2}$  and orbital angular momentum  $l_{\kappa}$  coupled up to  $j_{\kappa}$ :

$$\Phi_\kappa^m = \sum_{m_l, m_s} \langle l_\kappa \frac{1}{2} m_l m_s | j_\kappa m \rangle Y_l^{m_l} \chi_{m_s}, \quad (5)$$

and satisfy the relation  $\boldsymbol{\sigma} \cdot \hat{\mathbf{r}} \Phi_\kappa^m = \Phi_{-\kappa}^m$ . The sum in (4) is over all the eigenstates of angular momentum of a given energy  $\epsilon$  in the potential ( $\epsilon$  can be chosen at will because the only boundary condition imposed on each partial wave is that the wavefunction is regular at the origin.) The power of  $i$  is extracted to make the coefficients  $D_\kappa$  real. The radial functions  $u_{\kappa, \epsilon}(r)$  and  $v_{\kappa, \epsilon}(r)$  satisfy the Dirac equations

$$\begin{aligned} u' + \frac{\kappa + 1}{r} u + (\epsilon + g\sigma)v &= 0, \\ v' - \frac{\kappa - 1}{r} v - (\epsilon - g\sigma)u &= 0. \end{aligned} \quad (6)$$

The wavefunction (4), with an arbitrarily chosen energy, will not satisfy the boundary condition (1) for an arbitrary  $k$ . However for any  $k$  there will be an energy for which the boundary condition is satisfied, and conversely for a given energy, if it is not in a band gap, there will be a corresponding value of  $k$ . Finding the correspondence determines the dispersion relation  $\epsilon(k)$ . This was done as follows. The boundary condition (1) can be rewritten

$$e^{-ikR \cos \theta} \psi(R, \theta, \phi) - e^{ikR \cos \theta} \psi(R, \pi - \theta, \pi + \phi) = 0. \quad (7)$$

The exponentials can be expanded in terms of Legendre polynomials and spherical Bessel functions, and we substitute in the form (4) for  $\psi$ . If we multiply by the spherical harmonic  $Y_L^M$ , for any  $L$  and  $M = 0$  or  $-1$ , and integrate over solid angle, we obtain an equation for a linear combination of the coefficients  $D_\kappa$ . The set of these can be written as a matrix equation as follows, where the rows of the matrix are labelled by  $(L, M)$ :

$$\sum_{\kappa} \mathbf{M}_{(L, M)\kappa} D_\kappa = 0, \quad (8)$$

where

$$\mathbf{M}_{(L, M)\kappa}(k, \epsilon) = \mathbf{m}_{(L, M)\kappa}(k) \begin{Bmatrix} v_{\kappa, \epsilon}(R) \\ u_{\kappa, \epsilon}(R) \end{Bmatrix} \text{ for } \begin{cases} L \text{ even} \\ L \text{ odd} \end{cases} \quad (9)$$

and

$$\begin{aligned} \mathbf{m}_{(L, M)\kappa}(k) &= \sum_l j_l(kR) (2l+1) |\kappa - M|^{\frac{1}{2}} (\text{Sign}(\kappa))^M (-1)^{(l+\kappa+L)/2} \\ &\times \begin{pmatrix} l & L & l_\kappa \\ 0 & 0 & 0 \end{pmatrix} \begin{pmatrix} l & L & l_\kappa \\ 0 & M & -M \end{pmatrix}. \end{aligned} \quad (10)$$

Numerically, if we truncate the expansion of the wavefunction at  $2n$  terms, we use only the first  $n$  values of  $L$ , giving a  $2n \times 2n$  matrix. This matrix equation can hold for non-trivial  $D_\kappa$  only if  $\det(M(k, \epsilon)) = 0$ . In practice we search for the value of  $k$  which gives a vanishing determinant for a given  $\epsilon$ . The top of the band,  $k_t$ , corresponds to the highest value of  $\epsilon$  for which such a  $k$  can be found. A typical dispersion relation is shown in figure 1.

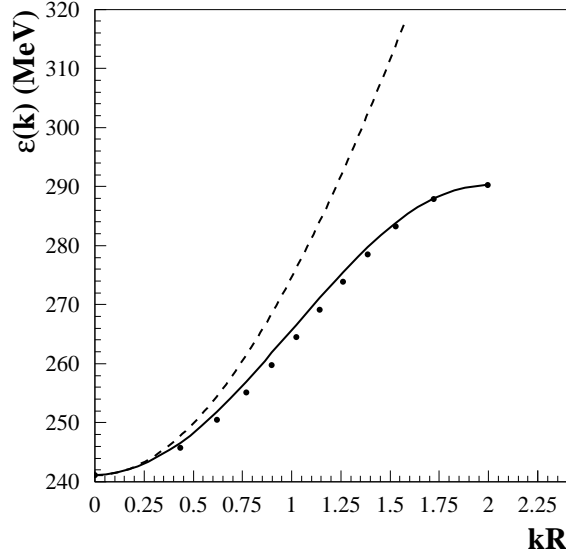


**Fig. 1:** Points: the dispersion relation for the F-L model with cell radius 1.5 fm. Solid curve: a sinusoidal fit to the data points. Dashed curve: the dispersion relation  $\epsilon(k) = \sqrt{e_b^2 + k^2}$  as assumed in Refs [4,7].

Having found the dispersion relation for  $\mathbf{k}$  along the  $z$ -axis, we know from spherical symmetry that it will be the same in any other direction. A simple rotation serves to produce the corresponding wavefunctions. The full scalar density is then spherically symmetric, and is given in terms of the  $\mathbf{k} = k\hat{\mathbf{z}}$  solutions by

$$\rho_s(r) = (3/k_t^3) \int_0^{k_t} k^2 \sum_{\kappa} D_{\kappa}^2 \left( u_{\kappa, \epsilon(k)}(r)^2 - v_{\kappa, \epsilon(k)}(r)^2 \right) dk. \quad (11)$$

The integration is done using Simpson's rule, with values of the integrand at regular values of  $k$  found by interpolation from the set of solutions, generally regularly spaced in  $\epsilon$ , which was used to find the dispersion relation. An overall normalisation constant has been included in the  $D_{\kappa}$ 's so that the corresponding vector density, integrated over the sphere, is three.

The scalar density then enters as a source term in the mean-field equation for the  $\sigma$  field. With a new field, the steps can be repeated until convergence is obtained. The total energy is then

$$E = (9/k_t^3) \int_0^{k_t} \epsilon(k) k^2 dk + 4\pi \int_0^R r^2 \left( \frac{1}{2} \sigma'(r)^2 + U(\sigma) \right) dr. \quad (12)$$

In everything above we have assumed that the band is filled right to the top. This is not in fact obvious. Isospin, spin and colour give each state a twelve-fold degeneracy, and there are only three quarks per soliton; the minimum energy state would therefore correspond to filling only the bottom quarter of the states. However such a filling would in no way correspond to the quarks in any one cell being coupled up to a colour singlet with the quantum numbers of the proton. Furthermore gluon exchange energies are comparable with

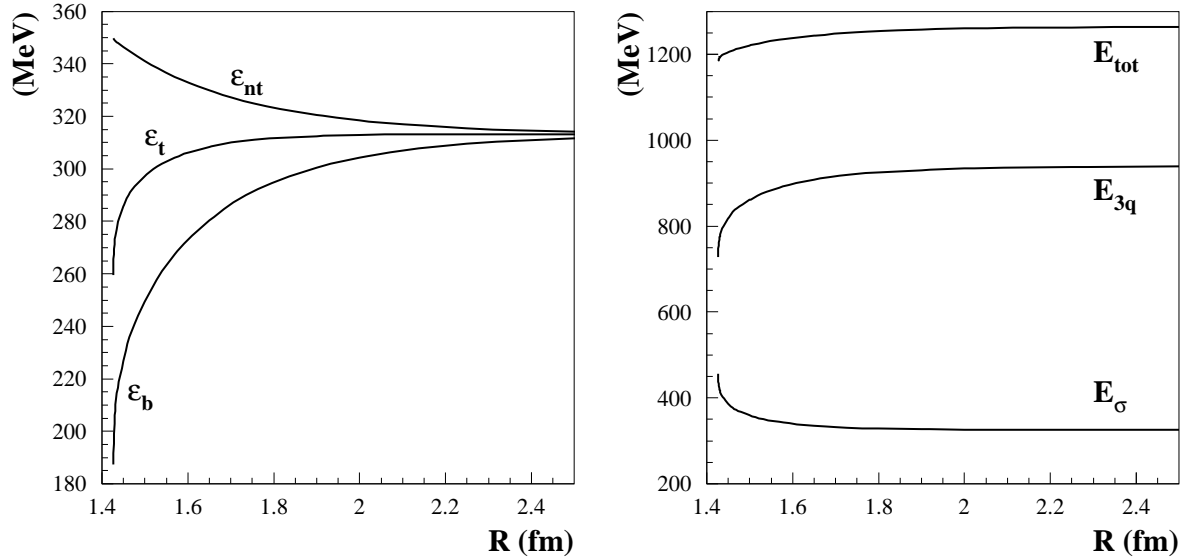


**Fig. 2:** The top and bottom of the band ( $\epsilon_t$  and  $\epsilon_b$ ) and the total energy  $E_{tot}$  along with its decomposition into quark ( $E_{3q}$ ) and mean field ( $E_{\sigma}$ ) parts. Also shown is the top of the band estimated by the method of [3] ( $\epsilon_{nt}$ ), which is not used in this calculation.

the width of the band, and so are capable of negating any saving in energy produced by a concentrated filling. Following ref. [3] we have used dilute filling.

In the case of the chiral quark-meson model the quark states are characterised by grand spin (sum of spin and isospin), and the filled quark band gives rise not only to a spherically symmetric quark density, but also an isovector pseudoscalar density. As required for self-consistency, this has indeed the hedgehog form  $\hat{r}_i \rho_h(r)$ . However in practical calculations the full scalar density in the F-L model was found to be very well approximated by truncating the sum over  $\kappa$  in (11) at the lowest value,  $\kappa = -1$ , and so in the chiral model we only used the  $G = 0$  states in calculating the source terms for the meson fields. The quark energy has the same form as Eq. (12), and the meson energy is

$$E_{\sigma\phi k} + E_{\sigma\phi p} = 4\pi \int_0^R r^2 \left( \frac{1}{2} \sigma'(r)^2 + \frac{1}{2} h'(r)^2 + U(\sigma, h) \right) dr. \quad (13)$$

The derivative and potential terms have been labeled separately for future reference. With hedgehog quarks the only degeneracy is due to colour, and so there is no ambiguity in the filling procedure; the band is filled to the top.

## IV. RESULTS

### A. Friedberg-Lee Model

Figure 2 shows the energy of a single cell as a function of cell radius. As the radius becomes large, the band width shrinks to zero and the total energy tends to the value for



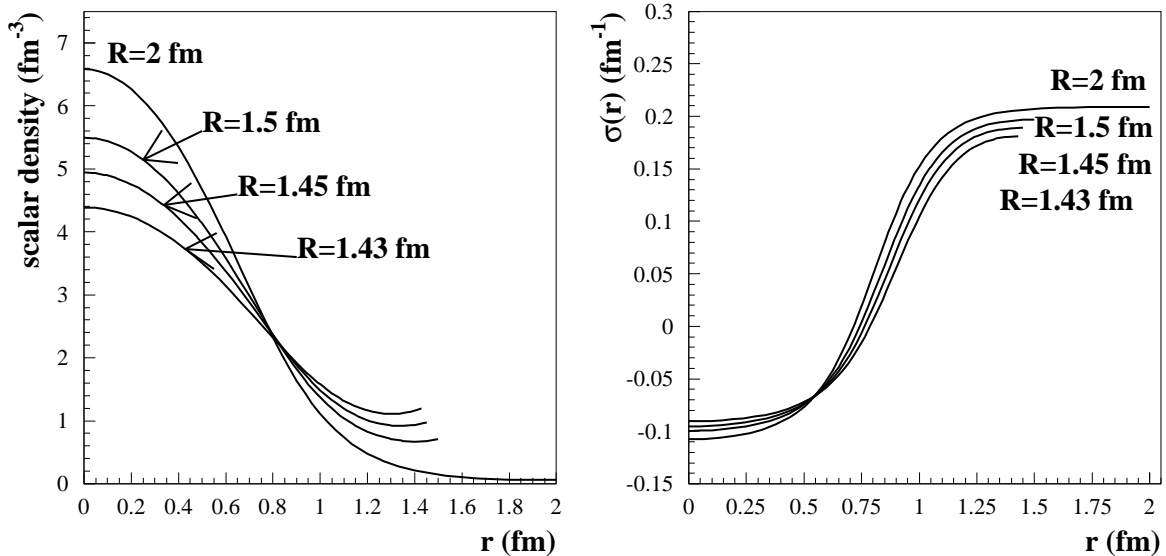


**Fig. 3:** The quark scalar density and meson field profiles for different radii in the F-L model.

an isolated soliton. As the radius decreases, the band widens. The bottom of the band falls fast, but the top falls too, and as a result the quark energy falls quite rapidly. The  $\sigma$  energy rises, but the overall energy drops.

Figure 3 helps to explain this: as the cell radius decreases, the mean radius of the quarks actually increases, with a corresponding decrease in kinetic energy which dominates the energy of the whole cell. We note also from figs 1 and 2 that the estimate of the top of the band given by the energy at which the upper component vanishes at the cell boundary ( $\epsilon_{nt}$ ), or by  $\sqrt{e_b^2 + (\pi/2R)^2}$ , is very different to that given by the self-consistent boundary conditions used here. This has a profound effect on the results, which are quite different.

Dodd and Lowe [12] have studied the one-dimensional F-L soliton crystal analytically. They found that the energy of the lowest-energy soliton state was very close to the energy of the massive-quark plasma, the difference becoming very small as the cell radius decreases. Unless the top state of the band was occupied, there was a radius at which the solution actually bifurcated from the plasma solution. In our calculations, however, the soliton solution is well below the massive plasma branch. The solution is finally lost at a radius of 1.427 fm, at which point it is clear from fig. 2 that the cell cannot be shrunk further. (At this point the band gap is still wider than the band.) This radius, at which the density is well below nuclear matter density, is disappointing. However it is not surprising. The Friedberg-Lee model has a massless plasma phase which is unrealistically low in energy (at a density corresponding to a radius of 1 fm, the massless plasma with a twelve-fold degeneracy of quark states has an energy of only 900 MeV per three quarks.) At the radius at which the solution is lost, a plasma with the same value of  $k_t$  is already of lower energy than our solution.

The calculation has also been done for the two parameter sets of ref. [2], which were tuned to give the same r.m.s. quark radius for the isolated soliton; the results were not

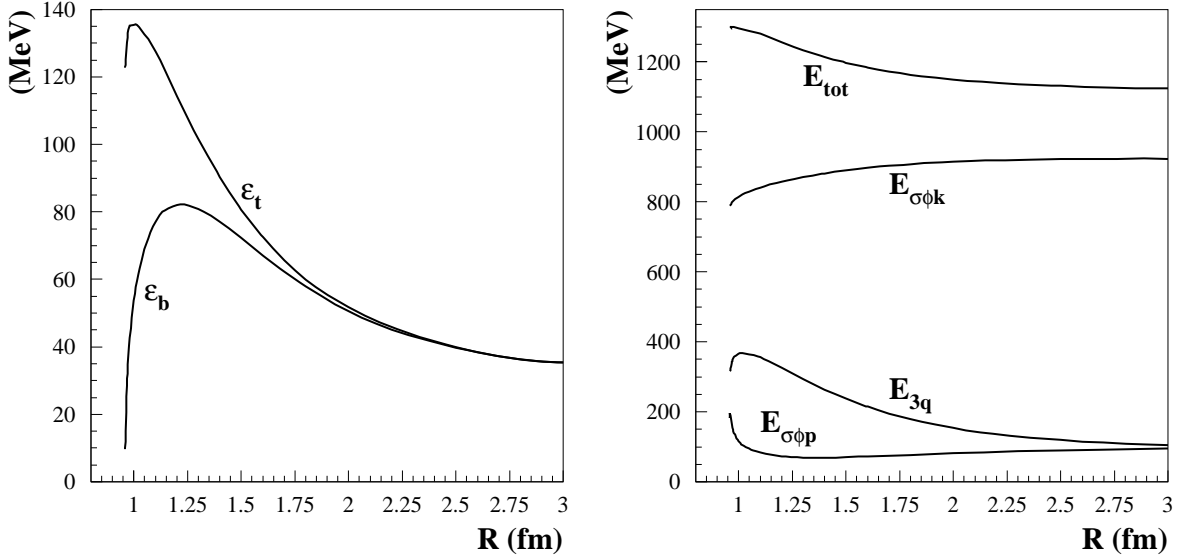


**Fig. 4:** The top and bottom of the band ( $\epsilon_t$  and  $\epsilon_b$ ) and the total energy ( $E_{tot}$ ) along with its decomposition into quark energy ( $E_{3q}$ ) and derivative and potential meson-field energies ( $E_{\sigma\phi k}$  and  $E_{\sigma\phi p}$ , Eq. (13)), in the chiral quark-meson model.

notably different.

It is worth commenting on the wavefunctions obtained with this method. Clearly it is of the essence that, for  $\mathbf{k} \neq 0$ , they are not pure  $s$ -waves, though in fact the admixtures of higher states are small. Nearly identical results are obtained if these are ignored in calculating the scalar density. However contrary to the assumption of ref. [7], the contributions of states with different  $k$  to the scalar density are markedly different, and as the high  $k$  states dominate because of the  $k^2$  factor, quite different results would be obtained if only the  $k = 0$  state were used.

## B. Chiral quark meson model

The behaviour of the chiral model (figs 4 and 5) is quite different from that of the Friedberg-Lee model. Until just below nuclear densities ( $R = 1.07$  fm), both the bottom and top of the band rise with decreasing radius, as does the total energy, in spite of the fact that the mesonic energy tends to fall. In contrast to the F-L model it can be seen that the mean radius of the quarks remains fairly constant, while the meson fields start to deviate from the chiral circle, increasing the potential energy of the quarks. One might expect the potential energy of the mesons ( $E_{\sigma\phi p}$ ) to rise also, but this is clearly offset by the decreasing volume of the cell. At nuclear densities there is a dramatic change in behaviour, as the quark energy falls sharply and the total energy starts to level off. At  $R = 0.958$  fm the solution is lost.

This time, when the solution vanishes, the plasma solution (with a uniform  $\sigma$  and zero pion field) is still much higher in energy, since the meson field are sitting at the top of

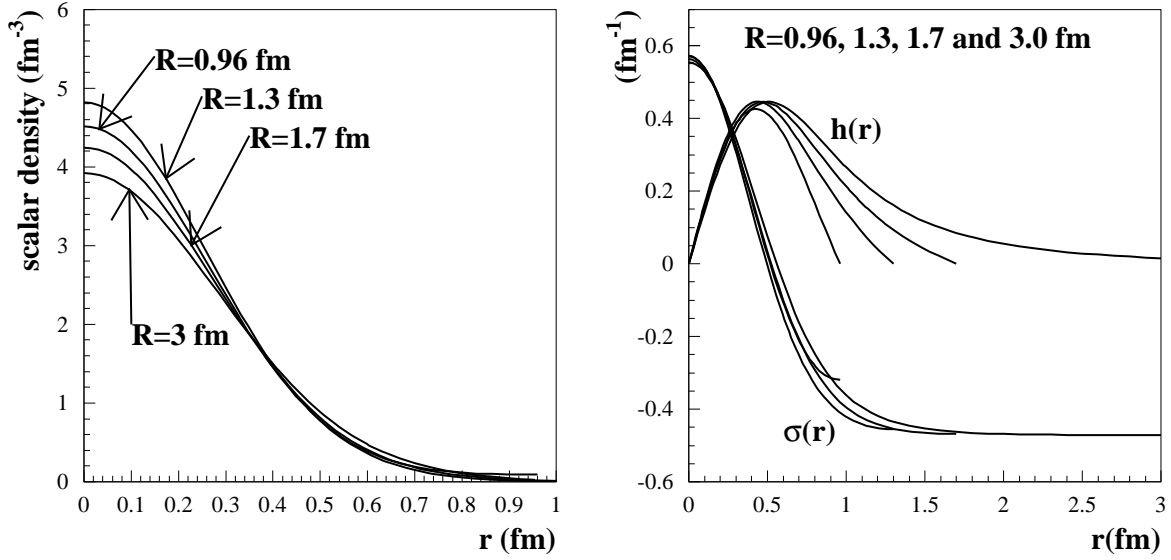


**Fig. 5:** The quark scalar density and meson field profiles for different radii.

the Mexican hat rather than approximately following the brim, as they do in the soliton. There are lower plasma states with plane-wave pion fields [14], but these do not satisfy our boundary conditions. However there may be another, plasma-like solution in which the meson fields do not wrap round the chiral circle but make an excursion round it before returning to their original values; the quarks would be in weakly-distorted plane-wave states. Since there would be no band gap, such a solution is cannot be found with our algorithm. Transition to this state would however represent deconfinement to a state of matter with a pion condensate, which therefore happens at 1.4 times nuclear density in this model.

In summary neither model shows the full behaviour expected of the energy-density curve, which is expected to have a long-range attraction and a short-range repulsion. In view of the many physical effects omitted (meson exchange, gluonic effects, fermi-motion of nucleons) and the deficiencies of the models used, this is perhaps not surprising.

## V. CONCLUSION

We have introduced a novel method of treating soliton matter in the Wigner-Seitz approximation which avoids the arbitrariness of previous treatments. By imposing a Bloch-like boundary condition—which however is independent of any crystal lattice—on the quarks in a spherically symmetric potential we can generate the dispersion relation complete with band gaps, and by filling a band we provide a spherically symmetric source for the field which gives rise to the potential. Thus for the first time a completely self-consistent treatment of the fields in the Wigner-Seitz cell is possible. The same boundary conditions are also satisfied by the uniform plasma solution which is the lowest energy state at high densities, and so this method is particularly suited to examining the deconfinement transition.

Many previous Wigner-Seitz calculations of soliton matter have been carried out. All

have found that the results are extremely sensitive to the choice of the top of the band. It is therefore very satisfactory to have a way of determining this self-consistently.

We have carried out calculations in the Friedberg-Lee and chiral quark-meson models. In the former no signs of repulsion are seen, and the solution disappears well below nuclear densities as the plasma solution takes over as the lowest energy state. In the latter short-range repulsion is seen, and the solution is lost at around 1.4 times nuclear density. Since the solitons in this case are hedgehogs, however, rather than nucleons, the relevance to nuclear matter remains to be elucidated.

## ACKNOWLEDGMENTS

J. McG. would like to thank M. Birse for useful conversations and suggestions. This work was supported in part by the UK EPSRC. U. W. was supported by the Studienstiftung des deutschen Volkes.

## APPENDIX: THE DISPERSION RELATION FOR HEDGEHOG QUARKS

The quantum number which commutes with the Dirac Hamiltonian in the chiral quark-meson model is grand spin, which is the sum of spin and isospin:  $\mathbf{G} = \mathbf{I} + \mathbf{j}$ . Eigenstates of grand spin have been constructed by Kahana and Ripka [13]. In the current case the projection of  $\mathbf{G}$  along  $\mathbf{k}$  is a good quantum number, and since we are interested in the band which develops from the isolated  $G = 0$  state, we need only consider  $M_G = 0$ . For a given  $G$  there are four distinct Dirac spinors, two of each parity, and the coupling to the mean fields mixes the same-parity pairs. Thus we can write down wavefunctions characterised by grand spin and parity: writing  $q_G$  for states with  $P = (-1)^G$  and  $p_G$  for states with  $P = (-1)^{G+1}$ , we have

$$q_G(\mathbf{r}) = \sqrt{\frac{1}{2}} \left[ \begin{pmatrix} u_1(r) \\ i\boldsymbol{\sigma} \cdot \hat{\mathbf{r}} v_1(r) \end{pmatrix} \left( \Phi_{-G-1}^{-\frac{1}{2}} u - \Phi_{-G-1}^{\frac{1}{2}} d \right) + \begin{pmatrix} f_1(r) \\ i\boldsymbol{\sigma} \cdot \hat{\mathbf{r}} g_1(r) \end{pmatrix} \left( \Phi_G^{-\frac{1}{2}} u + \Phi_G^{\frac{1}{2}} d \right) \right] \quad (\text{A1})$$

$$p_G(\mathbf{r}) = \sqrt{\frac{1}{2}} \left[ \begin{pmatrix} v_2(r) \\ i\boldsymbol{\sigma} \cdot \hat{\mathbf{r}} u_2(r) \end{pmatrix} \left( \Phi_{G+1}^{-\frac{1}{2}} u - \Phi_{G+1}^{\frac{1}{2}} d \right) + \begin{pmatrix} g_2(r) \\ i\boldsymbol{\sigma} \cdot \hat{\mathbf{r}} f_2(r) \end{pmatrix} \left( \Phi_{-G}^{-\frac{1}{2}} u + \Phi_{-G}^{\frac{1}{2}} d \right) \right] \quad (\text{A2})$$

and the radial function obey the following equations

$$\begin{aligned} v'_2 + \frac{G+2}{r} v_2 - (g\sigma \pm \epsilon) u_2 \pm (-v_2 \cos \theta + g_2 \sin \theta) gh &= 0 \\ u'_2 - \frac{G}{r} u_2 - (g\sigma \mp \epsilon) v_2 \mp (-u_2 \cos \theta + f_2 \sin \theta) gh &= 0 \\ g'_2 - \frac{G-1}{r} g_2 - (g\sigma \pm \epsilon) f_2 \pm (g_2 \cos \theta + v_2 \sin \theta) gh &= 0 \\ f'_2 + \frac{G+1}{r} f_2 - (g\sigma \mp \epsilon) g_2 \mp (f_2 \cos \theta + u_2 \sin \theta) gh &= 0 \end{aligned} \quad (\text{A3})$$

where  $\sin \theta = 2\sqrt{G(G+1)}/(2G+1)$  and  $\cos \theta = 1/(2G+1)$ . (In deriving these equations, one should note that the convention of ref. [13] for the spin-angle functions is different from ours, with the result that each element of their table for the matrix elements of  $\boldsymbol{\tau} \cdot \hat{\mathbf{r}}$  (Eq. A.5) should be multiplied by  $-1$  for use with our wavefunctions.) For the ground state,  $G = 0$ , there is only one, positive parity, state,  $q_0$ , and only  $u_1$  and  $v_1$  are non-zero. Now because each of the other wavefunctions is a sum of two spinors, there will be two linearly independent solutions of the same form, which we obtain by imposing two different boundary conditions at the origin; we choose to set each of the two lower components to zero in turn to get the two different solutions. This extra degree of freedom requires an extra index, so that we have, for  $G \neq 0$ ,  $q_G^n$ ,  $p_G^n$ , where  $n = 1, 2$ . In constructing a wavefunction to satisfy the boundary conditions (1) we use a superposition of states of all grand spin and parity:

$$\psi(\mathbf{r}, t) = \sum_G \sum_{n=1}^2 i^G (B_G^n q_G^n(\mathbf{r}) + C_G^n p_G^n(\mathbf{r})) e^{-i\epsilon t}. \quad (\text{A4})$$

The boundary condition on the wavefunction is the same as before. When imposed on (A4) the states with parity  $(-1)^G$  and those with  $(-1)^{G+1}$  decouple; since we want to consider the band based on the ground state  $G^P = 0^+$ , this means that we only need to include the  $(-1)^G$  states in (A4)—that is, only the  $q_G^n$ . The boundary condition then gives rise to the equation

$$\sum_G \sum_{n=1}^2 \mathbf{H}_{(L,M)(G,n)} B_G^n = 0 \quad (\text{A5})$$

where

$$\mathbf{H}_{(L,M)(G,n)}(k, \epsilon) = \begin{cases} \mathbf{m}_{(L,M)G}(k) g_1^{G,n}(\epsilon, R) - \mathbf{m}_{(L,M)-G-1}(k) v_1^{G,n}(\epsilon, R) \\ \mathbf{m}_{(L,M)G}(k) f_1^{G,n}(\epsilon, R) - \mathbf{m}_{(L,M)-G-1}(k) u_1^{G,n}(\epsilon, R) \end{cases} \text{ for } \begin{cases} L \text{ even} \\ L \text{ odd} \end{cases} \quad (\text{A6})$$

and  $\mathbf{m}$  is defined in Eq. (10).

## REFERENCES

- [1] M. K. Banerjee and J. A. Tjon, Phys. Rev. **C56** (1997) 497;  
K. Saito, K. Tsushima and A. W. Thomas, Phys. Rev. **C55** (1997) 2637 and references therein.
- [2] J. Achtzehnter, W. Scheid, and L. Wilets, Phys. Rev. **D32** (1985) 2414.
- [3] M. C. Birse, J. J. Rehr, and L. Wilets, Phys. Rev. **C38** (1988) 359.
- [4] B. Banerjee, N. K. Glendenning, and V. Soni, Phys. Lett. **155B** (1985) 213;
- [5] N. K. Glendenning and B. Banerjee, Phys. Rev. **C34** (1986) 1072.
- [6] L.R. Dodd, M. A. Lohe, and M. Rossi, Phys. Rev. **C36** (1987) 1573.
- [7] C. W. Johnson, G. Fai and M. R. Frank, Phys. Lett. **B386** (1996) 75;  
C. W. Johnson and G. Fai, `nuc1-th/9707054`.
- [8] E. Wigner and F. Seitz, Phys. Rev. **43** (1933) 804; **46** (1934) 509.
- [9] R. Friedberg and T. D. Lee Phys. Rev. **D15** (1977) 1694.
- [10] M. C. Birse and M. K. Banerjee, Phys. Lett. **136B** (1984) 284; Phys. Rev. **D31** (1985) 118.
- [11] S. Kahana, G. Ripka and V. Soni, Nucl. Phys. **A415** (1984) 351.
- [12] L. R. Dodd, Australian Journal of Physics, **44** (1991) 161;  
L.R. Dodd and M. A. Lohe, J. Math. Phys. **32** (1991) 1368;  
M. A. Lohe, Physica **D50** (1991) 259
- [13] S. Kahana and G. Ripka Nucl. Phys. **A429** (1984) 462.
- [14] M. Kutschera, W. Broniowski and A. Kotlorz, Phys. Lett. **237B** (1990) 159;  
Nucl. Phys. **A516** (1990) 566.